

# Geophysical Research Letters

## RESEARCH LETTER

10.1029/2018GL079901

### Key Points:

- Plant physiological responses drive a larger increase in the daily intensity of runoff than the annual mean in simulations with rising CO<sub>2</sub>
- Plant physiological responses to rising CO<sub>2</sub> contribute as much as radiative greenhouse effects to changes in the 99th percentile daily runoff
- Assessments of future flood risk on global scales should include both atmosphere and land-driven impacts on rainfall and runoff intensity

### Supporting Information:

- Supporting Information S1

### Correspondence to:

G. J. Kooperman,  
kooperman@uga.edu

### Citation:

Kooperman, G. J., Fowler, M. D., Hoffman, F. M., Koven, C. D., Lindsay, K., Pritchard, M. S., et al. (2018). Plant physiological responses to rising CO<sub>2</sub> modify simulated daily runoff intensity with implications for global-scale flood risk assessment. *Geophysical Research Letters*, 45, 12,457–12,466. <https://doi.org/10.1029/2018GL079901>

Received 26 FEB 2018

Accepted 25 OCT 2018

Accepted article online 31 OCT 2018

Published online 20 NOV 2018

## Plant Physiological Responses to Rising CO<sub>2</sub> Modify Simulated Daily Runoff Intensity With Implications for Global-Scale Flood Risk Assessment

Gabriel J. Kooperman<sup>1</sup> , Megan D. Fowler<sup>2</sup> , Forrest M. Hoffman<sup>3,4</sup> , Charles D. Koven<sup>5</sup> , Keith Lindsay<sup>6</sup> , Michael S. Pritchard<sup>2</sup> , Abigail L. S. Swann<sup>7,8</sup> , and James T. Randerson<sup>2</sup> 

<sup>1</sup>Department of Geography, University of Georgia, Athens, GA, USA, <sup>2</sup>Department of Earth System Science, University of California, Irvine, Irvine, CA, USA, <sup>3</sup>Computational Earth Sciences Group and Climate Change Science Institute, Oak Ridge National Laboratory, Oak Ridge, TN, USA, <sup>4</sup>Department of Civil and Environmental Engineering, University of Tennessee, Knoxville, TN, USA, <sup>5</sup>Climate and Ecosystem Sciences Division, Lawrence Berkeley National Laboratory, Berkeley, CA, USA, <sup>6</sup>Climate and Global Dynamics Division, National Center for Atmospheric Research, Boulder, CO, USA, <sup>7</sup>Department of Atmospheric Sciences, University of Washington, Seattle, WA, USA, <sup>8</sup>Department of Biology, University of Washington, Seattle, WA, USA

**Abstract** Climate change is expected to increase the frequency of flooding events and, thus, the risks of flood-related mortality and infrastructure damage. Global-scale assessments of future flooding from Earth system models based only on precipitation changes neglect important processes that occur within the land surface, particularly plant physiological responses to rising CO<sub>2</sub>. Higher CO<sub>2</sub> can reduce stomatal conductance and transpiration, which may lead to increased soil moisture and runoff in some regions, promoting flooding even without changes in precipitation. Here we assess the relative impacts of plant physiological and radiative greenhouse effects on changes in daily runoff intensity over tropical continents using the Community Earth System Model. We find that extreme percentile rates increase significantly more than mean runoff in response to higher CO<sub>2</sub>. Plant physiological effects have a small impact on precipitation intensity but are a dominant driver of runoff intensification, contributing to one half of the 99th and one third of the 99.9th percentile runoff intensity changes.

**Plain Language Summary** Floods are one of the most devastating natural disasters in the world, contributing to thousands of deaths and billions of dollars in damages annually. Climate change is expected to increase flood exposure considerably through the 21st century. However, recent studies assessing future flood risk on global scales by downscaling precipitation from Earth system models often neglect important plant physiological responses to rising CO<sub>2</sub>. In particular, higher CO<sub>2</sub> concentrations may lower stomatal conductance and, in the absence of significant plant growth, reduce water loss through transpiration, increasing soil moisture in many regions. For a given precipitation rate, higher soil moisture can decrease the amount of rain that infiltrates the soil and increase runoff. Here we apply a simulation design that isolates the independent effects of higher CO<sub>2</sub> on radiatively driven precipitation intensification from plant-driven soil moisture changes. We show that plant-physiological responses to increasing CO<sub>2</sub> are major drivers of the runoff intensity change in the tropics. Land surface changes contribute to one half of the 99th percentile runoff change and one third of the 99.9th percentile change. Our results suggest that comprehensive flood assessments should account for plant physiology as well as radiative impacts of higher CO<sub>2</sub> in order to better inform flood prediction and mitigation practice.

## 1. Introduction

Floods are the most frequently occurring natural disaster in the world. Hundreds of millions of people and trillions of US dollars in material assets are at risk of exposure to river flooding (Jongman et al., 2012), and current estimates of annual damages from flooding events exceed 100 billion US dollars (UNISDR, 2015). Future flood exposure could increase as much as 25 times by the end of the 21st century under business-as-usual emissions and medium population growth scenarios (Hirabayashi et al., 2013). However, many factors contribute to future flood risk (e.g., climate change, land-use change, population growth, and socioeconomic change) and assessments of its uncertainty (e.g., climate model biases, emissions scenarios, and downscaling methods), which have led to a large range in estimated changes across different studies (Alfieri et al., 2017;

Arnell & Gosling, 2016; Hirabayashi et al., 2013; Jongman et al., 2012; Winsemius et al., 2016). While many factors ultimately depend on human choices (e.g., fossil fuel consumption, population growth, and flood infrastructure), a better understanding of the physical processes that control these flooding events is needed to provide effective guidance for future policy decisions. In particular, it is critical to improve understanding of how greenhouse gas emissions can influence flood-related parameters (i.e., runoff and precipitation) that are used as inputs from global Earth system model (ESM) projections for high-resolution flood prediction and damage assessment studies.

Accurately assessing the impacts of changes in river flooding statistics over the next century requires a cross-disciplinary approach that accounts for atmospheric processes, land-surface hydrology, and socioeconomic conditions over a range of scales. Recent global-scale flood assessments have been based on a progression (cascade) of downscaling techniques that begin with low-resolution ( $\sim 1\text{--}2^\circ$ ) global forcing data (e.g., ESM output) downscaled through high-resolution ( $\sim 0.25\text{--}0.5^\circ$ ) hydrological or river routing models to estimate inundated area or flood volume (Pappenberger et al., 2012; Ward et al., 2013; Winsemius et al., 2013). These flood maps are then combined with local-scale ( $\sim 1$  km) physical (e.g., elevation and landscape) and socioeconomic (i.e., infrastructure and population) conditions to estimate changes in flood hazards and exposure. Although there are biases in the baseline representation of some important processes in ESMs (e.g., light precipitation is too frequent; Sun et al., 2006), biases are often assumed to be similar under historical and future conditions (Hirabayashi et al., 2013), and ESMs have been shown to capture relative changes consistent with theoretical expectations (Allen & Ingram, 2002; Pendergrass & Hartmann, 2014). Furthermore, downscaling can also account for processes with limited representation in ESMs (e.g., impacts of small-scale topography for local watersheds) and has been shown to produce fairly realistic river discharge statistics (Hirabayashi et al., 2013). However, while downscaling is necessary for connecting global changes simulated by ESMs to the scales relevant for human populations and property, ultimately the climate change signal at the end of the downscaling process depends on its inputs and, thus, the changes simulated within the coarse-resolution global model itself. Most often, the downscaling approach used by hydrologists is a one-way coupling, in which the high-resolution model does not respond directly to changes in greenhouse gas concentrations nor interact via feedbacks with the global ESM. In this study, we directly assess the ESM variables that serve as inputs to this downscaling process in order to better understand what drives the climate change impacts that have been identified in previous flood assessments.

Two methods are often applied to downscale ESM projections and represent basin-level hydrology in global-scale flood assessments. The first method is based on meteorological inputs, primarily ESM precipitation and temperature, to global hydrological models that estimate runoff, river flow, and inundation (Arnell & Gosling, 2016; Winsemius et al., 2016). Typically, the hydrological model framework applies a fixed set of land-surface conditions (including leaf area index, canopy interception capacity, and stomatal conductance), which do not respond interactively to changes in the atmospheric  $\text{CO}_2$  concentration (e.g., Mac-PDM [Gosling & Arnell, 2011] and GLOFRIS [Winsemius et al., 2013]). The second method is based on ESM runoff as a direct input to a river routing model (Hirabayashi et al., 2013), which allows nonstationary climate changes in atmosphere-vegetation coupling to occur interactively within the ESM (e.g., changes in stomatal conductance and leaf area) before downscaling for river flow and inundation (e.g., CaMa-Flood; Yamazaki et al., 2011). Both methods provide high-resolution global flood frequencies, and while there are benefits to the first method (e.g., simulated precipitation can be bias-corrected prior to estimating runoff), it neglects important plant-physiological responses to changes in atmospheric  $\text{CO}_2$  concentration, surface temperature, and humidity, which have been shown to influence runoff on long timescales (Betts et al., 2007; Swann et al., 2016). Thus, in this study we focus our analysis on *daily runoff intensity*, as the most important ESM input variable driving flood downscaling in the second method.

The climate system's response to rising  $\text{CO}_2$  can influence daily runoff in several direct and indirect ways. Total runoff includes contributions from both surface and subsurface runoff (infiltration and saturation excess), which depend on the precipitation rate at the surface over a range of timescales, infiltration rate, and soil moisture flow rate (Lawrence et al., 2011). Interactive dynamical influences on the infiltration and flow rates are largely determined by the soil water content, which is in turn constrained by water loss through evapotranspiration. Transpiration, the largest component of evapotranspiration in ecosystems with moderate to high leaf area, is limited by net radiation at the surface and stomatal conductance and therefore is

not an immediate sink for precipitation on daily timescales but instead influences the moisture content of the soil column on longer timescales (i.e., weeks to months). As a result, *daily runoff intensity* is determined by both the daily precipitation rate and the capacity of the soil column to absorb additional water. Even for a fixed precipitation rate, higher soil water content decreases the amount of water that can infiltrate the surface and increases the amount of runoff.

Mechanisms controlling the intensity of daily precipitation rates are strongly influenced by radiatively driven climate change (Allan & Soden, 2008), while total water storage is influenced by both radiative and plant physiological responses to rising CO<sub>2</sub> (Swann et al., 2016). Radiative responses in the tropics are expected to drive an intensification of extreme (99.9th percentile rates) precipitation at a rate of ~10%/°C (O’Gorman, 2012, 2015). Physiological responses are expected to reduce stomatal conductance (the aperture on leaves that controls gas exchange; Ball et al., 1987; Field et al., 1995; Medlyn et al., 2011), which can lead to less transpiration and higher soil moisture in some regions (Swann et al., 2016), though there is uncertainty with regard to how much this may be partially offset by increases in leaf area (Reich et al., 2014) or changes in water-use efficiency (Keeling et al., 2017). Both radiative and physiological effects can also influence surface-temperature/evaporative-demand (even for extremes; Skinner et al., 2018), atmospheric stability, circulation, and moisture convergence in ways that impact mean precipitation and evaporation patterns (Kooperman et al., 2018; Pu & Dickinson, 2014) and, thus, soil moisture and runoff. For a detailed summary of the ways in which radiative (Figure S1A in the supporting information) and physiological (Figure S1B) processes can influence daily runoff intensity, see the supporting information (Text S1 and Figure S1).

In this study, we separate the relative contributions of atmospheric-driven radiative-greenhouse effects from land-driven plant-physiological effects on runoff and precipitation intensity changes under increasing CO<sub>2</sub> at daily timescales. Through this analysis we show that plant physiological effects contribute significantly to increases in runoff intensity with first-order implications for flood risk analysis. The remainder of the paper is organized into three main sections summarizing the model and simulations, major results, and conclusions of this work.

## 2. Model and Simulations

This study analyzes output from the Community Earth System Model with biogeochemistry (CESM1-BGC; Hurrell et al., 2013; Lindsay et al., 2014). In this configuration, CESM is fully coupled with interactive atmosphere (CAM4; Neale et al., 2010), land (CLM4; Lawrence et al., 2011), ocean (POP2; Smith et al., 2010), and sea-ice (CICE4; Hunke & Lipscomb, 2008) components. Precipitation in CAM4 is generated by parameterizations of deep convection, shallow convection, and large-scale prognostic cloud processes (Neale et al., 2010). In CLM4, evapotranspiration includes components from transpiration, ground evaporation, and canopy evaporation. Transpiration is controlled by stomatal conductance, which is represented by the Ball-Berry model as a function of gross photosynthesis, atmospheric CO<sub>2</sub> concentration, surface relative humidity, temperature, and atmospheric pressure (Ball et al., 1987; Oleson et al., 2010). Total runoff includes contributions from surface runoff, which is a function of saturation and infiltration excess, and subsurface runoff, which is a function of impermeable area and water table depth (Lawrence et al., 2011). CLM4 has regional runoff biases due to uncertainties in the representation of precipitation and subgrid soil infiltration/flow, but the biases are comparable in magnitude to other ESMs (Du et al., 2016), and the annual mean and annual cycle has improved significantly relative to previous versions (Lawrence et al., 2011; Oleson et al., 2008).

To separate the contributions of radiative and physiological effects on daily precipitation and runoff intensity, we conducted four simulations with CESM following the methodology of the carbon-climate feedback experiments in CMIP5 (Arora et al., 2013), which has been applied previously to investigate hydrological sensitivities to rising CO<sub>2</sub>, including drought (Swann et al., 2016) and precipitation (Kooperman et al., 2018; Pu & Dickinson, 2014; Skinner et al., 2017). All four simulations began from a spun-up preindustrial climate (i.e., CO<sub>2</sub> concentration of 285 ppm), and one simulation continued this setup for an additional 50 years to provide preindustrial background conditions (i.e., preindustrial simulation). In the remaining simulations, the CO<sub>2</sub> concentration increased from 285 to 1140 ppm (quadrupled CO<sub>2</sub>) at a rate of 1%/year over 140 years and was then held constant at the quadrupled CO<sub>2</sub> concentration for an additional 50 years (Figure S1). In one simulation, both radiation and terrestrial vegetation experienced increasing levels of CO<sub>2</sub> (i.e., Full simulation). In the other two simulations, the radiative (i.e., radiation simulation) and physiological (i.e., Physiology simulation,

including impacts on stomatal conductance and leaf area) responses were isolated by holding the CO<sub>2</sub> concentration at a constant preindustrial level in the land-surface and atmosphere, respectively.

Our primary analysis focused on daily runoff directly from these CESM simulations in order to develop an understanding of the dominant processes controlling changes in response to increasing CO<sub>2</sub>. This follows from our hypothesis that the climate change signal obtained in downscaled flood impact studies originates from the changes in critical input variables simulated at the ESM scale. To test this view, we also assessed the changes in total river discharge when CESM runoff was downscaled using the Catchment-Based Macroscale Floodplain model (CaMa-Flood). CaMa-Flood is a global-scale hydrodynamic river routing model that can be driven by ESM runoff, which represents river channel, floodplain, and inundation dynamics (Yamazaki et al., 2011). In this study, CaMa-Flood was configured at 0.25° horizontal resolution, which has been shown to produce mean annual and annual maximum daily discharge rates comparable in magnitude to Global Runoff Data Centre observations when driven by CMIP5 runoff (Figure S1 from Hirabayashi et al., 2013). We analyzed the last 10 years of each CESM simulation and compared the quadrupled CO<sub>2</sub> simulations to the preindustrial simulation both directly and after downscaling with CaMa-Flood for the results shown below.

### 3. Results and Discussion

Plant-physiological effects alone, driven by reduced stomatal conductance, have been shown to significantly increase global mean runoff in response to a doubling of atmospheric CO<sub>2</sub> (6% in Betts et al., 2007, and 8.4% in Cao et al., 2010), contributing to more than half of the total increase from physiological and radiative effects together (11% and 14.9%, respectively). In this study, we focus on quadrupled CO<sub>2</sub> climate change in the tropics (23°S to 23°N), where the relative contribution from physiological effects is more than 90% of the total mean annual increase (Table S1). Tropical annual mean runoff increases by nearly 40% ( $0.47 \pm 0.06$  mm/day, mean change with 90% confidence interval based on interannual variability) in the Full simulation, 38% ( $0.45 \pm 0.05$  mm/day) in the Physiology simulation, and only 4% ( $0.04 \pm 0.06$  mm/day) in the Radiation simulation. In the Full simulation, changes in runoff are relatively large compared to changes in mean precipitation over tropical land, which increases by only 8% ( $0.30 \pm 0.10$  mm/day). The precipitation change in the Full simulation is driven by both radiation (4%;  $0.15 \pm 0.09$  mm/day) and physiology (3%;  $0.11 \pm 0.07$  mm/day). Additionally, the radiative effects of increasing CO<sub>2</sub> are the primary driver of a mean increase in surface temperature over tropical land, with 4.8, 4.3, and 0.6 °C increases in the Full, Radiation, and Physiology simulations, respectively. Thus, while radiative effects are the dominant component of the mean surface temperature change in the tropics, physiological effects contribute comparably to the mean precipitation change and are the main component of a substantial mean runoff increase.

Even though the tropical mean precipitation change is slightly larger in the Radiation simulation, the spatial pattern of the change in the Full simulation is more reflective of the physiological response (Figures 1a–1c), particularly over tropical forest regions due to a physiologically driven reduction in evapotranspiration (Figures S2D–S2F) and both positive (over Indonesia) and negative (over South America) moisture convergence anomalies (Kooperman et al., 2018). The spatial pattern of the mean runoff change largely reflects the precipitation change, with an increase over Asia, Central Africa, and the Andes and a decrease over the Amazon and Central America in the Full simulation (Figures 1d–1f). This pattern is consistent with the CMIP5 multimodel mean for RCP8.5 (Berg et al., 2017) and CO<sub>2</sub>-only (Swann et al., 2016) scenarios as represented by the change in mean precipitation minus evaporation. The magnitudes of the mean runoff increases are however greater than the mean precipitation increases in the Full and Physiology simulations, leading to a larger tropics-wide increase in runoff than in precipitation (i.e., 40% and 38% relative to 8% and 3%, respectively). In contrast, runoff and precipitation both increase by approximately 4% in the Radiation simulation, with similar regional patterns across tropical land.

Associated with large increases in mean runoff in the Full and Physiology simulations, CESM simulates increases in total water storage (Figures S2A–S2C) and soil moisture (Figure S3). Near the surface (Figures S3D–S3F), reduced evapotranspiration in the Physiology simulation leads to a widespread increase in soil moisture across tropical land, with the exception of lowland Amazon forests, where precipitation declines. Deeper water storage increases most significantly along the eastern slope of the Andes and southern edge of the Sahel. Increases in near surface soil moisture reduce infiltration rates, and increases in deep water storage reduce the capacity of the soil column to absorb additional water, which contribute to increases in mean

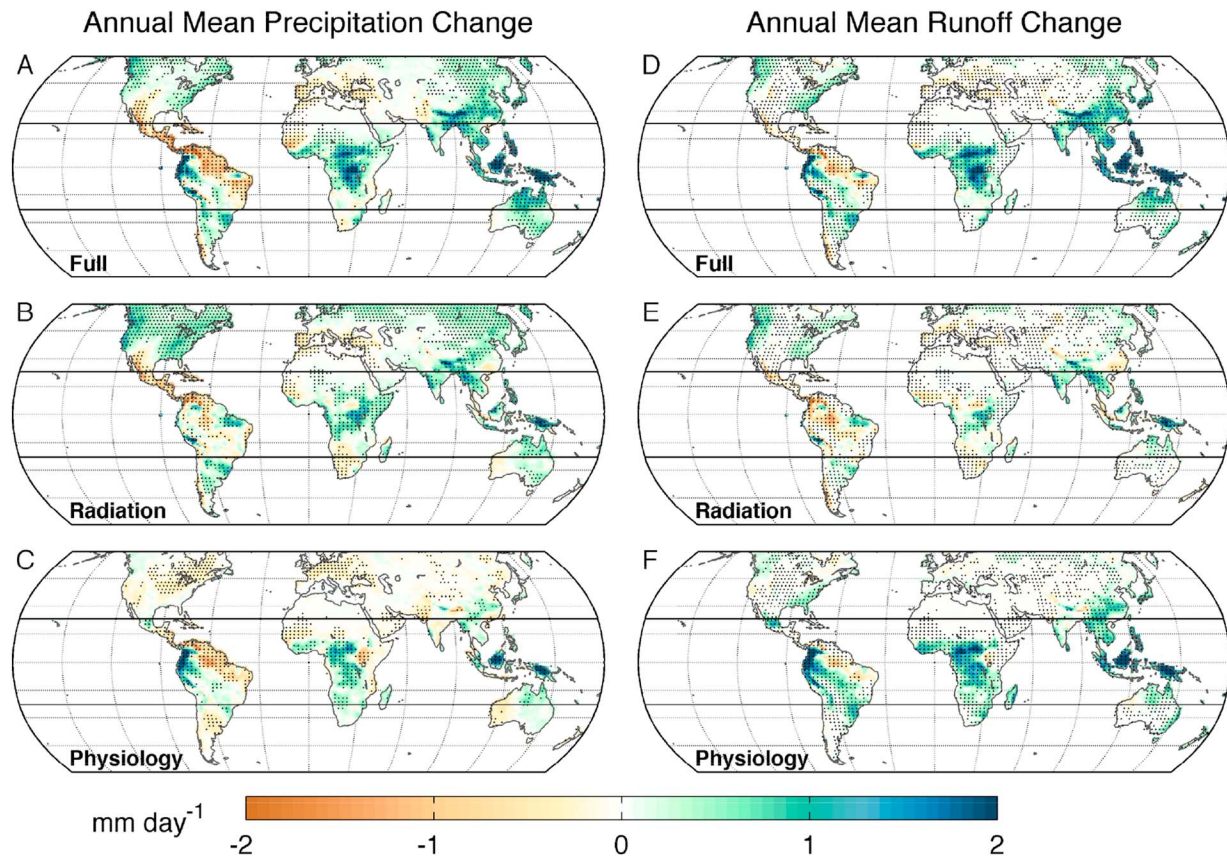


**Figure 1.** Annual mean (a–c) precipitation and (d–f) runoff rate change ( $4\times\text{CO}_2$  minus preindustrial  $\text{CO}_2$  climate) from the (a, d) Full, (b, e) Radiation, and (c, f) Physiology simulations. Horizontal lines delineate the tropics between  $23^\circ\text{S}$  and  $23^\circ\text{N}$ . Stippling shows significance at 90% confidence based on interannual variability.

surface and ground water runoff, respectively. In the Radiation simulation, soil moisture decreases across the entire tropics, even in regions where precipitation increases, with the exception of the Somali peninsula. Decreases in soil moisture in the Radiation simulation result in part from an increase in evaporative demand driven by higher surface temperatures (Scheff & Frierson, 2014) that increase water loss through evapotranspiration (Figure S2E). The physiological effects are larger than radiative effects in the tropics, leading to drying in the Amazon and wetting in the Andes, Central Africa, and Asia in the Full simulation. This pattern is generally consistent with patterns of soil moisture change in the CMIP5 RCP8.5 multimodel mean, with the exception of the increase in the Andes, which is not evident in the RCP8.5 simulations, possibly due to a stronger relative physiological forcing with  $4\times\text{CO}_2$  or a CESM-specific response (Berg et al., 2017).

The impacts of physiology on runoff averaged over long periods of time (e.g., annual timescales) are consistent with evidence from earlier modeling studies (Betts et al., 2007; Cao et al., 2010; Lemordant et al., 2018; Swann et al., 2016) and observations (Gedney et al., 2006). However, impacts on shorter timescales (i.e., daily) that are relevant to flooding events have received less attention. The daily intensity of runoff from CESM in the tropics increases by 49% ( $4.06 \pm 0.02$  mm/day) as measured by changes in the 99th percentile rate and by 75% for the 99.9th percentile rate in the Full simulation (Table S1 and Figures 2a and 2c). For runoff percentiles greater than the 90th, percentage increases exceed the annual mean change. Percentage increases in extreme runoff rates are more than twice that of precipitation, which increases by only 21% ( $5.72 \pm 0.34$  mm/day) for the 99th percentile rate. For both runoff and precipitation, the Full simulation (blue line) is nearly a linear combination (dashed orange line) of the physiological (green line) and radiative (red line) effects simulated separately. Physiology contributes to a small increase in precipitation intensity ( $0.89 \pm 0.59$  mm/day for the 99th percentile rate), as demonstrated by Skinner et al. (2017), but a much larger increase in runoff intensity ( $2.13 \pm 0.18$  mm/day for the 99th percentile rate), with a continuous response as

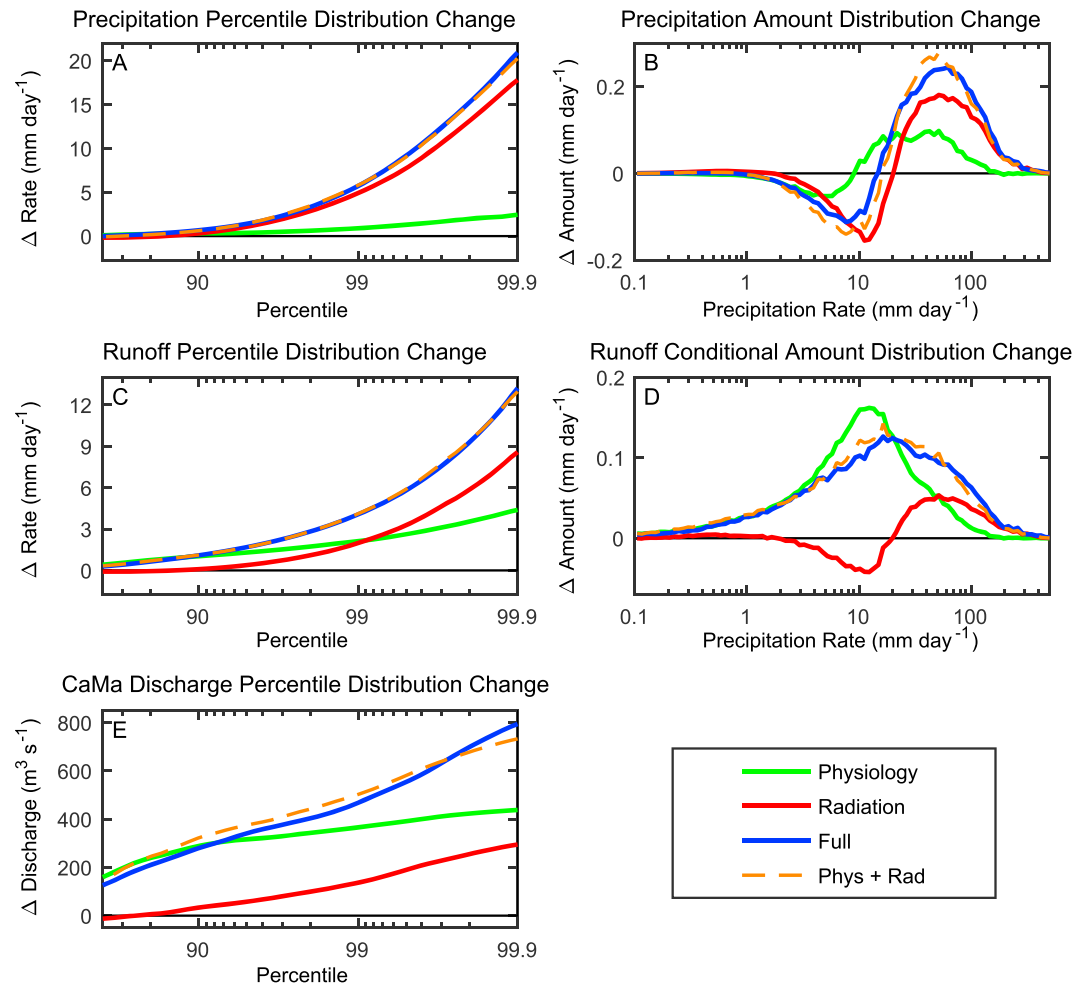


**Figure 2.** Daily (a, c, e) percentile rate distribution change and (b, d) amount distribution change ( $4\times\text{CO}_2$  minus preindustrial  $\text{CO}_2$  climate) as a function of the daily precipitation rate for (a, b) precipitation, (c, d) runoff, and (e) CaMa-Flood downscaled discharge averaged over tropical ( $23^\circ\text{S}$  to  $23^\circ\text{N}$ ) land from the (blue) Full, (red) Radiation, and (green) Physiology simulations. Runoff is shown as a (d) conditional amount distribution, which represents the amount of runoff as a function of the precipitation rate. The orange dashed line is a linear combination of the change from Radiation and Physiology simulations together. The units of the (b, d) amount distributions are in mm/day but have been scaled by  $\Delta\ln R^{-1}$  in order to remain independent of bin spacing, where  $\Delta\ln R = \Delta R/R$  with bin center  $R$  and bin width  $\Delta R$ . With logarithmic spacing,  $\Delta\ln R$  is a constant value (equal to 0.1 here) with units of  $\text{mm}\cdot\text{day}^{-1}/\text{mm}\cdot\text{day}^{-1}$  and is thus a unitless scaling term; see Kooperman et al. (2016) for more details.

$\text{CO}_2$  raises through the simulation (Figure S4). This equates to a physiological contribute of 52% of the 99th percentile rate change and 33% of the 99.9th percentile rate change from the Full simulation (Table S1).

Consistent with our working hypothesis, changes in runoff statistics translate directly into corresponding changes in downscaled flood statistics. When CESM runoff is aggregated downstream by means of offline downscaling with CaMa-Flood, preindustrial conditions produce annual mean river discharge rates that are comparable in magnitude to present-day observations (associated with daily precipitation rates that are comparable but slightly weaker than observations over tropical land; Figure S5) and the discharge rates increase significantly in response to higher  $\text{CO}_2$  (Figures 2e and S6E). The physiological component is dominant through the 99.9th percentile, confirming its importance for hydrological extremes when the processes of river and floodplain dynamics are better represented. This signal is also not unique to CESM. Alternative representations of model physics also confirm the important role of physiology in the Canadian Earth System Model (CanESM2; von Salzen et al., 2013), in which the physiological contribution to runoff percentile rate changes averaged over the tropics is the dominant component to even higher percentiles than in CESM (Figure S7B). As discussed above, our simulation design follows the carbon-climate feedbacks CMIP5

experiment, which included contributions from eight modeling centers. However, only CanESM2 saved daily runoff output at quadrupled CO<sub>2</sub>, so a full multimodel intercomparison is not possible at this time.

Changes in runoff intensity are closely related to the changes in precipitation intensity when radiative effects are simulated alone, as demonstrated in the precipitation and conditional runoff amount distributions (Figures 2b and 2d; baseline distributions are shown in Figures S6B and S6D). These distributions show the amount of total precipitation and runoff associated with daily precipitation rates discretized with logarithmic bin spacing (Kooperman et al., 2016; Pendergrass & Hartmann, 2014). All simulations shift toward more intense precipitation rate distributions (centered between 10 and 20 mm/day), indicating more precipitation from heavier rates and less from lighter rates (Figure 2b). The shift is larger in the Full and Radiation simulations, suggesting that radiative effects primarily drive the intensification. Physiological effects play an important role in influencing mean precipitation changes but have a smaller influence on the intensity of precipitation. The change in the runoff distribution from the Radiation simulation has the same shape as precipitation—there is more precipitation generated from heavy rates, resulting in more runoff associated with heavy rain rate days.

Runoff intensity changes in the Full and Physiology simulations are fundamentally different from precipitation changes (Figure 2d). More runoff is associated with all precipitation rates regardless of whether or not there is more accumulated precipitation at those rates. Even though the amount of rainfall from light precipitation rates decreases, the amount of runoff associated with light precipitation days increases. The increase in runoff associated with the physiological response is much larger than the decrease in rainfall associated with the radiative response for precipitation rates less than approximately 20 mm/day, leading to an increase in runoff in the Full simulation at all precipitation rates. For precipitation rates greater than 20 mm/day, radiative effects contribute to increases in runoff, making the combined response (i.e., the Full simulation) greater than the Physiology or Radiation simulations alone. For the tropical average, radiative impacts only become the dominant driver of runoff changes when precipitation rates exceed approximately 50 mm/day, about the 99.9th percentile precipitation rate in the preindustrial climate. The combined radiative and physiological effects (orange dashed line) generally recreate the amount distribution in the Full simulation.

Spatially, extreme runoff increases most across the tropics, where the precipitation intensity (O’Gorman, 2012, 2015) and physiological responses over tropical forests (Kooperman et al., 2018; Swann et al., 2016) can both be significant. Patterns of 99th percentile precipitation (Figures 3a–3c) and runoff (Figures 3d–3f) rate changes are similar to mean changes in CESM, highlighting the largest increases over the Andes, Central Africa, Asia, and Northern Australia in the Full and Physiology simulations. CanESM2, in contrast, primarily highlights the Central African action center (Figures S7C–S7E). Radiative effects contribute to the changes in runoff intensity in most of these regions as well in CESM, with the exception of the Andes where runoff intensity decreases and the eastern Amazon where precipitation and runoff intensity increases. Radiative effects also contribute to increases in precipitation intensity over most middle and high latitude lands, which is partially offset by a decrease in intensity associated with the physiological response. Physiological effects also contribute to a decrease in precipitation intensity over the northeast coast of South America, which leads to a small decrease in runoff in the same region. Despite contributing to a reduction in precipitation intensity outside of the tropics, the Physiology simulation has little runoff intensity change poleward of 23°, and while precipitation intensity increases broadly over middle and high latitudes in the Full and Radiation simulations, runoff intensity increases are isolated to a few regions (e.g., west coast of North America and China). Outside of these regions, increases in evapotranspiration (Figures S2D and S2E) appear to reduce near surface soil moisture (Figures S3D and S3E) and allow for more infiltration.

The spatial patterns of lower percentile rate changes (e.g., ninetieth percentile; Figure S8) reflect the mean changes, but for higher percentiles (e.g., 99.9th percentile; Figure S9), most regions have either an increase in intensity or no change. For precipitation, the 99.9th percentile rates increase by more than 30 mm/day across most of the tropics and 10–15 mm/day in higher latitudes. Like the 99th percentile, the 99.9th percentile runoff changes occur mostly in the tropics and northern China. As shown for tropics-wide changes (Table S1 and Figure 2), the radiative impacts on precipitation begin to contribute more to runoff intensification at higher percentiles (i.e., 99.9th) than plant-physiological effects. The largest and most widespread 99.9th percentile runoff changes, with increases over 30 mm/day, are seen over Asia, including the Maritime Continent, India, Southeast Asia, China, and Northern Australia. Runoff and precipitation intensity increases in these

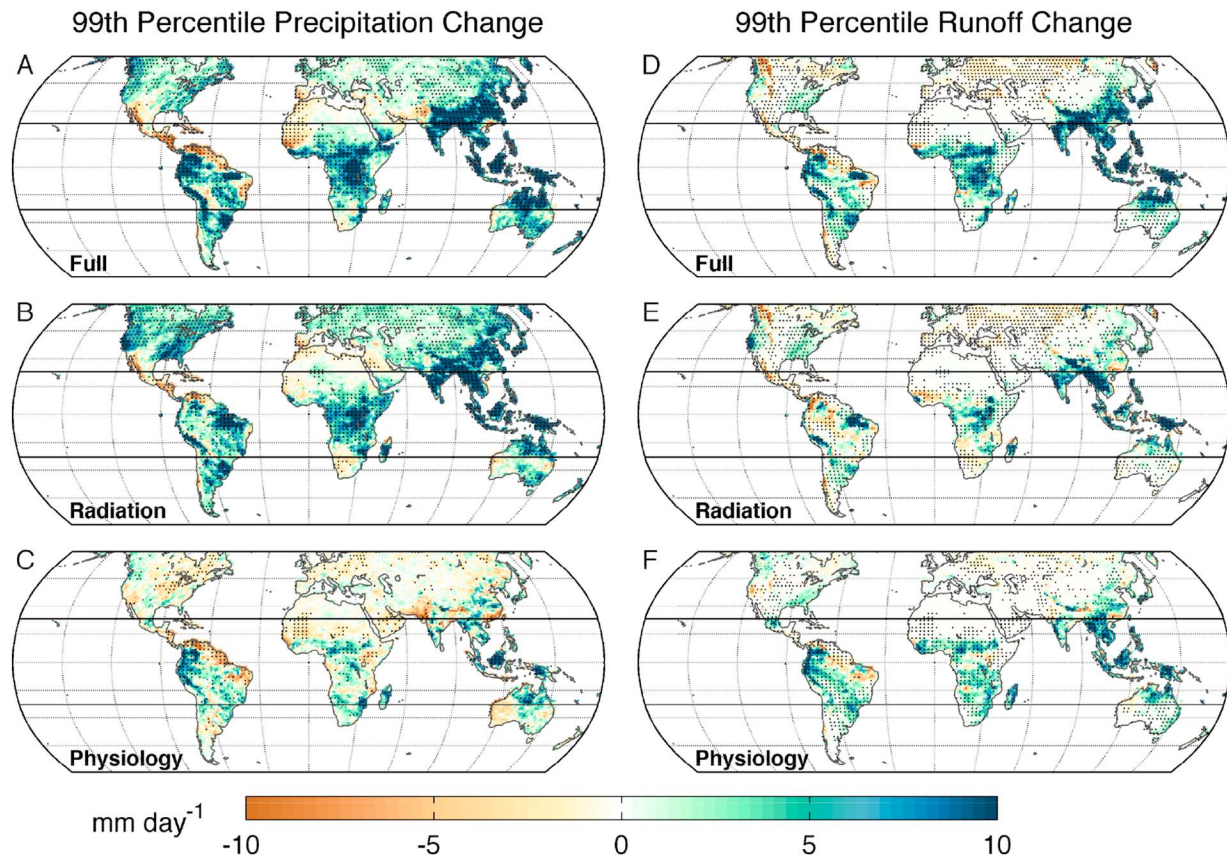


**Figure 3.** Daily 99th percentile (a–c) precipitation and (d–f) runoff rate change ( $4\times\text{CO}_2$  minus preindustrial  $\text{CO}_2$  climate) from (a, d) Full, (b, e) Radiation, and (c, f) Physiology simulations. Horizontal lines delineate the tropics between  $23^\circ\text{S}$  and  $23^\circ\text{N}$ . Stippling shows significance at 90% confidence based on interannual variability.

regions are strongly affected by both radiative and physiological responses to rising  $\text{CO}_2$  and are thus most likely to experience greater flooding in the future.

#### 4. Conclusions

Previous work has demonstrated that plant physiological effects can contribute significantly to increases in annual mean runoff, particularly in the tropics (Betts et al., 2007; Gedney et al., 2006). By isolating the physiological and radiative responses to rising  $\text{CO}_2$ , here we show that physiological effects in CESM can impact runoff intensity on daily timescales by a higher percentage than the annual mean and are therefore a major mechanism that controls the physical processes (i.e., soil infiltration and flow rates) leading to extreme flooding events. In the tropical average, reduced stomatal conductance increases soil moisture, leading to more runoff from all precipitation rates, such that precipitation events that may not cause flooding in the present climate may produce new runoff extremes in the future. Therefore, even without significant changes in precipitation intensity, flooding risk could increase as a result of vegetation responses to rising  $\text{CO}_2$  alone. In combination with expected increase in precipitation intensity, future runoff intensity is likely to increase substantially. Our results indicate that radiatively driven intensification of precipitation and plant physiological influences on soil moisture contribute equally to increases in the 99th percentile runoff rates in the tropics. Radiative effects play a larger role for less frequent runoff events (greater than the 99th percentile) at the extreme tail of the distribution, but physiological effects remain important by increasing soil moisture and amplifying flood risks from precipitation intensification.

Our results demonstrate that future flood risk assessments based on downscaling ESM results using hydrological and/or river routing models are strongly influenced not only by  $\text{CO}_2$  effects on precipitation and temperature within the atmosphere but also by plant responses that influence soil moisture. Therefore,

improving projections of future flood risk requires reducing uncertainty in the representation of plant processes (e.g., plant growth and stomatal conductance responses to rising CO<sub>2</sub>) as well as the effects of climate change on precipitation. Multimodel intercomparisons focused on evaluating plant processes and understanding their roles in the hydrological cycle may help reduce uncertainty in ESM projections. Furthermore, in addition to improved prediction, a better understanding of the physical processes that impact runoff intensity will inform adaptation, monitoring, and infrastructure development strategies. To mitigate future damage and deaths associated with river flooding, better monitoring of soil moisture conditions may be necessary, as well as preservation of ecosystems that support greater water retention (e.g., wetlands). The intensification of precipitation associated with the Madden Julian Oscillation and monsoons (Kooperman et al., 2016), radiatively and physiologically driven increases in mean precipitation from enhanced moisture convergence (Kooperman et al., 2018), and rising soil moisture from reduced stomatal conductance may make the Maritime Continent and Southeast Asia particularly vulnerable to future flooding.

#### Acknowledgments

G. J. K. and J. T. R. acknowledge support from the Gordon and Betty Moore Foundation (GBMF3269), UC Irvine's Office of Research, and NASA's SMAP program. C. D. K., F. M. H., M. D. F., M. S. P., and J. T. R. acknowledge support from the U.S. Department of Energy (DOE) Office of Science Biological and Environmental Research programs. The DOE support includes funding from the Regional and Global Climate Modeling program through the Reducing Uncertainties in Biogeochemical Interactions through Synthesis and Computation (RUBISCO) Scientific Focus Area and from the Terrestrial Ecosystem Sciences program through the Next Generation Ecosystem Experiments (NGEE)—Tropics as well as the Early Career Award Program (DE-SC0012152). K. L. acknowledges support from the National Center for Atmospheric Research (NCAR), which is sponsored by the US National Science Foundation (NSF). A. L. S. S. acknowledges support from the NSF (AGS-1321745 and AGS-1553715). CESM development is led by NCAR and supported by NSF and DOE. CESM simulations were run and archived at the NCAR Computational and Information Systems Laboratory on Yellowstone (P36271028). This experiment branched from CMIP5 ESM simulations that are available on the Earth System Grid: Full (1pctCO<sub>2</sub>, <https://doi.org/10.1594/WDCC/CMIP5.NFCBc1>), Radiation (esmFdbk1, <https://doi.org/10.1594/WDCC/CMIP5.NFCBe1>), and Physiology (esmFixClim1, <https://doi.org/10.1594/WDCC/CMIP5.NFCBx1>). The extended daily output needed to recreate the figures in the manuscript are available at <http://kooperman.uga.edu/grl2018> or on request from the corresponding author.

#### References

- Alfieri, L., Bisselink, B., Dottori, F., Naumann, G., de Roo, A., Salamon, P., et al. (2017). Global projections of river flood risk in a warmer world. *Earth's Future*, 5, 171–182. <https://doi.org/10.1002/2016EF000485>
- Allan, R. P., & Soden, B. J. (2008). Atmospheric warming and the amplification of precipitation extremes. *Science*, 321(5895), 1481–1484. <https://doi.org/10.1126/science.1160787>
- Allen, M. R., & Ingram, W. J. (2002). Constraints on future changes in climate and the hydrologic cycle. *Nature*, 419(6903), 224–232. <https://doi.org/10.1038/nature01092>
- Arnell, N. W., & Gosling, S. N. (2016). The impacts of climate change on river flood risk at the global scale. *Climatic Change*, 134(3), 387–401. <https://doi.org/10.1007/s10584-014-1084-5>
- Arora, V. K., Boer, G. J., Friedlingstein, P., Eby, M., Jones, C. D., Christian, J. R., et al. (2013). Carbon-concentration and carbon-climate feedbacks in CMIP5 Earth system models. *Journal of Climate*, 26(15), 5289–5314. <https://doi.org/10.1175/JCLI-D-12-00494.1>
- Ball, J. T., Woodrow, I. E., & Berry, J. A. (1987). A model predicting stomatal conductance and its contribution to the control of photosynthesis under different environmental conditions. In J. Biggins (Ed.), *Progress in photosynthesis research* (pp. 221–224). Netherlands: Springer. [https://doi.org/10.1007/978-94-017-0519-6\\_48](https://doi.org/10.1007/978-94-017-0519-6_48)
- Berg, A., Sheffield, J., & Milly, P. C. D. (2017). Divergent surface and total soil moisture projections under global warming. *Geophysical Research Letters*, 44, 236–244. <https://doi.org/10.1002/2016GL071921>
- Betts, R. A., Boucher, O., Collins, M., Cox, P. M., Falloon, P. D., Gedney, N., et al. (2007). Projected increase in continental runoff due to plant responses to increasing carbon dioxide. *Nature*, 448(7157), 1037–1041. <https://doi.org/10.1038/nature06045>
- Cao, L., Bala, G., Caldeira, K., Nemani, R., & Ban-Weiss, G. (2010). Importance of carbon dioxide physiological forcing to future climate change. *Proceedings of the National Academy of Sciences of the United States of America*, 107(21), 9513–9518. <https://doi.org/10.1073/pnas.0913000107>
- Du, E., Di Vittorio, A., & Collins, W. D. (2016). Evaluation of hydrologic components of Community Land Model 4 and bias identification. *International Journal of Applied Earth Observation and Geoinformation*, 48, 5–16. <https://doi.org/10.1016/j.jag.2015.03.013>
- Field, C. B., Jackson, R. B., & Mooney, H. A. (1995). Stomatal responses to increased CO<sub>2</sub>: Implications from the plant to the global scale. *Plant, Cell & Environment*, 18(10), 1214–1225. <https://doi.org/10.1111/j.1365-3040.1995.tb00630.x>
- Gedney, N., Cox, P. M., Betts, R. A., Boucher, O., Huntingford, C., & Stott, P. A. (2006). Detection of a direct carbon dioxide effect in continental river runoff records. *Nature*, 439(7078), 835–838. <https://doi.org/10.1038/nature04504>
- Gosling, S. N., & Arnell, N. W. (2011). Simulating current global river runoff with a global hydrological model: Model revisions, validation, and sensitivity analysis. *Hydrological Processes*, 25(7), 1129–1145. <https://doi.org/10.1002/hyp.7727>
- Hirabayashi, Y., Mahendran, R., Koirala, S., Konoshima, L., Yamazaki, D., Watanabe, S., et al. (2013). Global flood risk under climate change. *Nature Climate Change*, 3(9), 816–821. <https://doi.org/10.1038/nclimate1911>
- Hunke, E. C., and Lipscomb, W. H. (2008). CICE: The Los Alamos sea ice model user's manual version 4, Los Alamos National Laboratory Tech. Rep. (LA-CC-06-012), pp 1–76.
- Hurrell, J., Holland, M. M., Gent, P. R., Ghan, S., Kay, J. E., Kushner, P. J., et al. (2013). The Community Earth System Model: A framework for collaborative research. *Bulletin of the American Meteorological Society*, 94(9), 1339–1360. <https://doi.org/10.1175/BAMS-D-12-00121.1>
- Jongman, B., Ward, P. J., & Aerts, J. C. J. H. (2012). Global exposure to river and coastal flooding: Long term trends and changes. *Global Environmental Change*, 22(4), 823–835. <https://doi.org/10.1016/j.gloenvcha.2012.07.004>
- Keeling, R. F., Graven, H. D., Welp, L. R., Resplandy, L., Bi, J., Piper, S. C., et al. (2017). Atmospheric evidence for a global secular increase in carbon isotopic discrimination of land photosynthesis. *Proceedings of the National Academy of Sciences*, 114(39), 10361–10366. <https://doi.org/10.1073/pnas.1619240114>
- Kooperman, G. J., Chen, Y., Hoffman, F. M., Koven, C. D., Lindsay, K., Pritchard, M. S., et al. (2018). Forest response to rising CO<sub>2</sub> drives zonally asymmetric rainfall change over tropical land. *Nature Climate Change*, 8(5), 434–440. <https://doi.org/10.1038/s41558-018-0144-7>
- Kooperman, G. J., Pritchard, M. S., Burt, M. A., Branson, M. D., & Randall, D. A. (2016). Impacts of cloud superparameterization on projected daily rainfall intensity climate changes in multiple versions of the Community Earth System Model. *Journal of Advances in Modeling Earth Systems*, 8, 1727–1750. <https://doi.org/10.1002/2016MS000715>
- Lawrence, D. M., Oleson, K. W., Flanner, M. G., Thornton, P. E., Swenson, S. C., Lawrence, P. J., et al. (2011). Parameterization improvements and functional and structural advances in version 4 of the Community Land Model. *Journal of Advances in Modeling Earth Systems*, 3, M030001. <https://doi.org/10.1029/2011MS000045>
- Lemordant, L., Gentine, P., Swann, A. S., Cook, B. I., & Scheff, J. (2018). Critical impact of vegetation physiology on the continental hydrologic cycle in response to increasing CO<sub>2</sub>. *Proceedings of the National Academy of Sciences*, 115(16), 4093–4098. <https://doi.org/10.1073/pnas.1720712115>
- Lindsay, K., Bonan, G. B., Doney, S. C., Hoffman, F. M., Lawrence, D. M., Long, M. C., et al. (2014). Pre-industrial-control and twentieth-century carbon cycle experiments with the Earth system model CESM1(BGC). *Journal of Climate*, 27(24), 8981–9005. <https://doi.org/10.1175/JCLI-D-12-00565.1>

- Medlyn, B. E., Duursma, R. A., Eamus, D., Ellsworth, D. S., Prentice, I. C., Barton, C. V. M., et al. (2011). Reconciling the optimal and empirical approaches to modeling stomatal conductance. *Global Change Biology*, *17*(6), 2134–2144. <https://doi.org/10.1111/j.1365-2486.2010.02375.x>
- Neale, R. B., Richter, J. H., Conley, A. J., Park, S., Lauritzen, P. H., Gettelman, A., et al. (2010). Description of the NCAR Community Atmosphere Model (CAM 4.0) (NCAR Technical Note: NCAR/TN-485+STR). Boulder, CO: National Center for Atmospheric Research.
- O’Gorman, P. A. (2012). Sensitivity of tropical precipitation extremes to climate change. *Nature Geoscience*, *5*(10), 697–700. <https://doi.org/10.1038/ngeo1568>
- O’Gorman, P. A. (2015). Precipitation extremes under climate change. *Current Climate Change Reports*, *1*(2), 49–59. <https://doi.org/10.1007/s40641-015-0009-3>
- Oleson, K. W., Niu, G.-Y., Yang, Z.-L., Lawrence, D. M., Thornton, P. E., Lawrence, P. J., et al. (2008). Improvements to the Community Land Model and their impact on the hydrological cycle. *Journal of Geophysical Research*, *113*, G01021. <https://doi.org/10.1029/2007JG000563>
- Oleson, K. W., Lawrence, D. M., Bonan, G. B., Flanner, M. G., Kluzek, E., Lawrence, P. J., et al. (2010). Technical Description of version 4.0 of the Community Land Model (CLM) (NCAR Technical Note: NCAR/TN-478+STR). Boulder, CO: National Center for Atmospheric Research.
- Pappenberger, F., Dutra, E., Wetterhall, F., & Cloke, H. L. (2012). Deriving global flood hazard maps of fluvial floods through a physical model cascade. *Hydrology and Earth System Sciences*, *16*(11), 4143–4156. <https://doi.org/10.5194/hess-16-4143-2012>
- Pendergrass, A. G., & Hartmann, D. L. (2014). Changes in the distribution of rain frequency and intensity in response to global warming. *Journal of Climate*, *27*(22), 8372–8383. <https://doi.org/10.1175/JCLI-D-14-00183.1>
- Pu, B., & Dickinson, R. E. (2014). Hydrological changes in the climate system from leaf responses to increasing CO<sub>2</sub>. *Climate Dynamics*, *42*(7–8), 1905–1923. <https://doi.org/10.1007/s00382-013-1781-1>
- Reich, P. B., Hobbie, S. E., & Lee, T. D. (2014). Plant growth enhancement by elevated CO<sub>2</sub> eliminated by joint water and nitrogen limitation. *Nature Geoscience*, *7*(12), 920–924. <https://doi.org/10.1038/ngeo2284>
- Scheff, J., & Frierson, D. M. W. (2014). Scaling potential evapotranspiration with greenhouse warming. *Journal of Climate*, *27*(4), 1539–1558. <https://doi.org/10.1175/JCLI-D-13-00233.1>
- Skinner, C. B., Poulsen, C. J., Chadwick, R., Diffenbaugh, N. S., & Fiorella, R. P. (2017). The role of plant CO<sub>2</sub> physiological forcing in shaping future daily-scale precipitation. *Journal of Climate*, *30*(7), 2319–2340. <https://doi.org/10.1175/JCLI-D-16-0603.1>
- Skinner, C. B., Poulsen, C. J., & Mankin, J. S. (2018). Amplification of heat extremes by plant CO<sub>2</sub> physiological forcing. *Nature Communications*, *9*(1094), 1–11.
- Smith, R., Jones, P., Briegleb, B., Bryan, F., Danabasoglu, G., Dennis, J., et al. (2010). The parallel ocean program (POP) Reference Manual (LANL Tech. Rep. LAUR-10–01853, p. 140). Los Alamos, NM: Los Alamos National Laboratory.
- Sun, Y., Solomon, S., Dai, A., & Portmann, R. W. (2006). How often does it rain? *Journal of Climate*, *19*(6), 916–934. <https://doi.org/10.1175/JCLI3672.1>
- Swann, A. L. S., Hoffman, F. M., Koven, C. D., & Randerson, J. T. (2016). Plant responses to increasing CO<sub>2</sub> reduce estimates of climate impacts on drought severity. *Proceedings of the National Academy of Sciences of the United States of America*, *113*(36), 10,019–10,024. <https://doi.org/10.1073/pnas.1604581113>
- UNISDR (2015). *Making development sustainable: The future of disaster risk management. Global Assessment Report on Disaster Risk Reduction 2015*. Geneva, Switz: United Nations Office for Disaster Risk Reduction (UNISDR).
- von Salzen, K., Scinocca, J. F., McFarlane, N. A., Li, J., Cole, J. N. S., Plummer, D., et al. (2013). The Canadian Fourth Generation Atmospheric Global climate Model (CanAM4). Part I: Representation of physical processes. *Atmosphere-Ocean*, *51*(1), 104–125. <https://doi.org/10.1080/07055900.2012.755610>
- Ward, P. J., Jongman, B., Weiland, F. S., Bouwman, A., van Beek, R., Bierkens, M. F. P., et al. (2013). Assessing flood risk at the global scale: Model setup, results, and sensitivity. *Environmental Research Letters*, *8*(4), 044019. <https://doi.org/10.1088/1748-9326/8/4/044019>
- Winsemius, H. C., Aerts, J. C. J. H., van Beek, L. P. H., Bierkens, M. F. P., Bouwman, A., Jongman, B., et al. (2016). Global drivers of future river flood risk. *Nature Climate Change*, *6*(4), 381–385. <https://doi.org/10.1038/nclimate2893>
- Winsemius, H. C., Van Beek, L. P. H., Jongman, B., Ward, P. J., & Bouwman, A. (2013). A framework for global river flood risk assessments. *Hydrology and Earth System Sciences*, *17*(5), 1871–1892. <https://doi.org/10.5194/hess-17-1871-2013>
- Yamazaki, D., Kanae, S., Kim, H., & Oki, T. (2011). A physically based description of floodplain inundation dynamics in a global river routing model. *Water Resources Research*, *47*, W04501. <https://doi.org/10.1029/2010WR009726>